Rainbow trapping within graded array of C-shaped cylinders

Jin Xu, De-zhi Ning, Li-fen Chen

State Key Laboratory of Coastal and Offshore Engineering, Dalian University of Technology, Dalian, 116024, China. Email addresses: xuj@mail.dlut.edu.cn; dzning@dlut.edu.cn; lifen_chen@dlut.edu.cn.

1. Introduction

Rainbow trapping phenomenon can induce an effect that enables the spatial separation and deceleration of broadband wave signals into their spectral components [1]. It was initially studied in optics [2] and later expanded to acoustics [3], elastic waves [4], seismic waves [5] and water waves [6]. This interesting phenomenon offers a potential pathway toward innovative technological applications ranging from enhanced acoustic filters to the advanced coastal protection strategies and efficient harvesting of wave energy.

The concept of rainbow trapping was firstly introduced to the field of water waves by Peter et al. [7], using an ordinary cylinder array with graded spacings. This was later verified experimentally by Archer et al. [8], who observed the occurrence of rainbow trapping within a similar graded ordinary cylinder array. Subsequently, Bennetts et al. [6] also observed this phenomenon within a C-shaped cylinder array with graded radii.

Despite the terminology of 'rainbow trapping' being applied broadly to both graded ordinary cylinder and C-shaped arrays, the underlying principles are different in the works of Archer et al. [8] and Bennetts et al. [6]. The difference originates from the type of resonances that the uniform periodic ordinary and C-shaped cylinder arrays can induce. For a uniform periodic ordinary cylinder array, the resonance occurring within the array must be Bragg resonance, while Bragg and local resonances could both occur in a uniform periodic C-shaped cylinder array.

If the array grading is sufficiently gradual, waves would behave locally as if they are propagating over a uniform array [6]. Hence, local resonance or Bragg resonance could occur within the local 'uniform' array. As the parameters (could be radii or spacings) in the array gradually change, the resonant frequencies at the different local 'uniform' array also change. It makes it possible for different-frequency wave to be blocked at different positions in the array due to the occurrence of resonance within different local 'uniform' array in the graded array. The rainbow trapping phenomenon can be seen as the occurrence of local or Bragg resonance for broadband waves at different local positions. Hence, it is logical to classify the phenomenon of rainbow trapping into two categories, i.e., rainbow trapping induced by local resonance and Bragg resonance, respectively.

To the best of the authors' knowledge, it is the first time to distinguish these two rainbow trapping phenomena in water wave based on their respective underlying mechanism. In this work, two type of rainbow trapping pheneomena are investigated using the Computational Fluid Dynamics (CFD) model based on OpenFOAM software, and the underlying mechanism is illustrated.

2. Model validation

To validate the numerical model, the experiments conducted by Dupont et al. [9] are reproduced using CFD model. The six C-shaped cylinders were configured in two rows and three columns along the walls of the wave flume in the experiment as shown in Fig. 1. The distance between adjacent C-shaped cylinders is uniform in both the x and y directions, with $a = b = 0.65$ m, and the water depth is $h = 0.5$ m. Each cylinder features an outer radius $R_1 = 0.15$ m and an inner radius $R_2 = 0.145$ m, with an opening length $l_n = 0.16$ m. A consistent wave steepness $H/L = 0.02$ was employed across all the wave periods, where H represents the wave height and L denotes the wavelength of the incident waves.

Given the symmetric nature of both the structure and flow field, the numerical simulation only considers half of the wave flume to conserve computational resources. The simulation domain measures

13.5 m in length and 0.325 m in width, while the centers of the three C-shaped cylinders are positioned at x = 5.10 m, 5.75 m, and 6.40 m, respectively. Waves are generated on the left boundary. To minimize the reflected waves at the left and right ends of wave flume, relaxation zones of one and two wavelengths are set to the two ends, respectively.

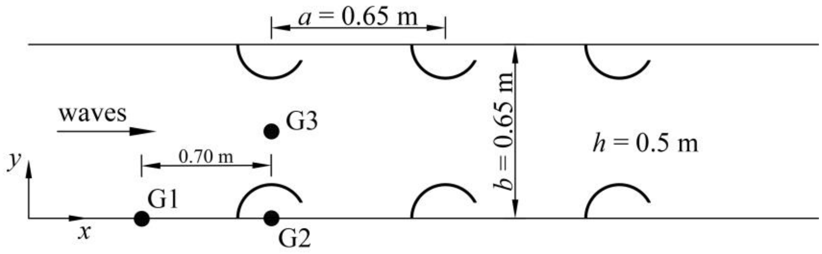

Fig.1 The layout of the array of C-shaped cylinder (top view).

The reflection coefficents R_s and transimission coefficents T_s obtained by the numerical model are compared with experiment measurement, as shown in Fig. 2. It can be seen from the figure, the results of the numerical model are in very good agreement with the experimental ones, comfirming the accuracy and the capability of the numerical model to predict the transmission and reflection coefficients within a C-shaped cylinder aray.

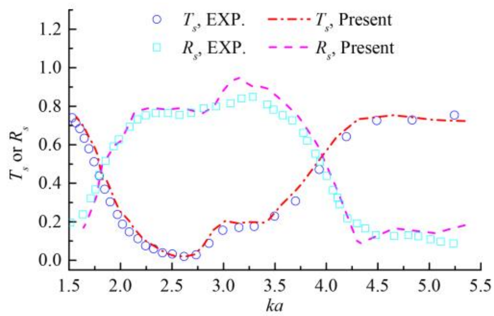

Fig. 2 Comparison of numerical results of the transmission and reflection coefficients with experimental data.

To distinguish the occurrence of local resonance and Bragg resonance, the validated case is employed as an example to display the modes of these two types of resonance. Fig. 3 (a) shows the non-dimensional surface elevations contours η' (= $\eta/H/2$) around the C-shaped cylinder array at ka = 3.57. It can be seen that the wave crests are acting on the first and third cylinders, while the wave trough is acting on the second cylinder, which is a typical Bragg resonance mode.

For local resonance, according to Hu et al. [10], when it occurs, the phase difference between waves inside and outside the cavity of C-shaped cylinder is close to π. Fig. 3 (b) shows the surface elevations contours at ka = 2.61. It can be observed from the figure that there is a significant phase difference between the inside and outside of the first C-shaped cylinder, with the waves inside and outside the cavity being in their trough and crest, respectively. Hence, in subsequent sections, the aforementioned characteristics are utilized to distinguish the occurrence of Bragg and local resonances.

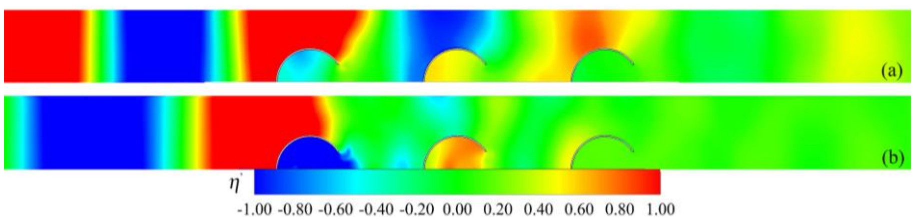

Fig. 3 The non-dimensional surface elevation contours around the graded array at (a) *ka* = 3.57 and (b) 3.62.

3. Results and discussions

Two different cases that rainbow trapping can occur within the array are investigated in this work. There are six C-shaped cylinders in the array for both two cases, and they are labeled as cylinder *A* - *F*. Case 1 is achieved by changing the radii of the C-shaped cylinders in the array as shown in Fig. 4 (a). The radius of each C-shaped cylinder is labeled as $R_{1,j}$, where j = 1, 2, 3, … , 6. The first C-shaped cylinder has an outer radius of 0.15 m, and the latter cylinder has a radius 0.02 m greater than the former, i.e. $R_{1,j+1} - R_{1,j} = 0.02$ m (about 13.3% of $R_{1,1}$). All the C-shaped cylinders have the same wall thickness of $w_n = 0.015$ m. The spacings between each two adjacent C-shaped cylinders are $a = 0.65$ m, and the width of the wave flume is $b = 0.65$ m. Case 2 is achieved by changing the spacings between two adjacent C-shaped cylinders in the array as shown in Fig. 4 (b). The radius of the C-shaped cylinder in the array is $R_1 = 0.21$ m, and is constant for all cylinders. The wall thickness is still $w_n = 0.015$ m. The spacings between two adjacent cylinders in the graded array are labeled as a_j, where j = 1, 2, 3, 4, 5. The first spacing a_1 is 0.65 m, and $a_{j+1} - a_j = 0.09$ m (about 13.8% of a_1).

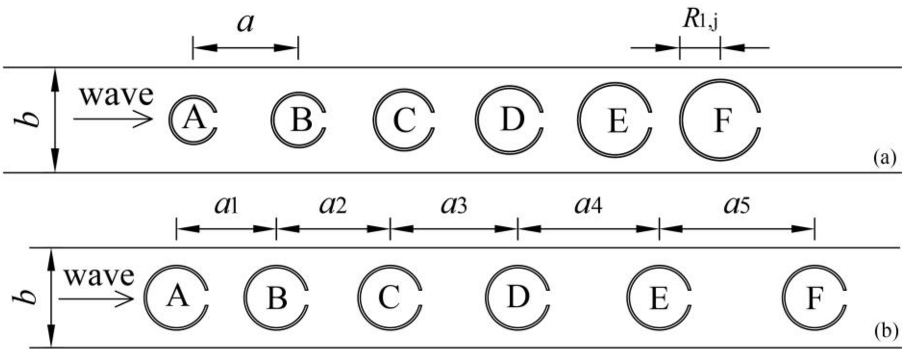

Fig. 4 The sketch of two proposed cases.

The non-dimensional surface elevation contours around the graded array at *ka* = 1.99 and 1.23 for Case 1 are shown in Fig. 5. It can be clearly seen from the figure that there is a phase difference between waves inside and outside Cylinder *B* at *ka* = 1.99 and Cylinder *E* at *ka* = 1.23, respectively. The local resonance occurs around Cylinder *B* at *ka* = 1.99 and Cylinder *E* at *ka* = 1.23, respectively. It can be seen from the figure that the position where local resonance occurs moves with the changes of incident wave frequency. This observation indicates that the phenomenon of rainbow trapping in Case 1 is indeed caused by local resonance.

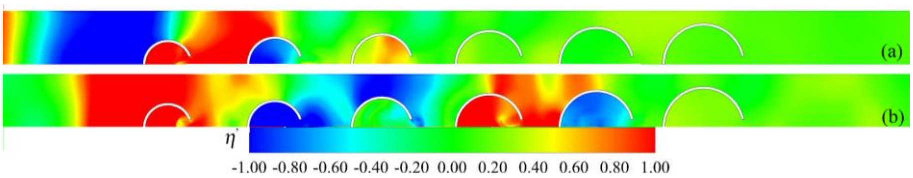

Fig. 5 The non-dimensional surface elevation contours around the graded array at *ka* = (a) 1.99 and (b) 1.23 for Case 1.

The non-dimensional surface elevation contours around the C-shaped cylinder array at *ka* = 4.18 and 2.93 for Case 2 are shown in Fig. 6. The Bragg resonance mode is identifiable near cylinders *A* - *C* at *ka* = 4.18, and cylinders *B* - *D* at *ka* = 2.93. It can be seen from the figure that the position where the Bragg resonance occurs moves with the changes of incident wave frequency, indicating that the rainbow trapping phenomenon of Case 2 is mainly caused by Bragg resonance. More results and conclusions will be shown in the workshop.

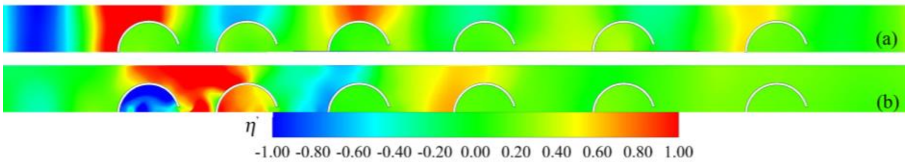

Fig. 6 The non-dimensional surface elevation contours around the graded array at *ka* = (a) 4.18 and (b) 2.93 for Case 2.

ACKNOWLEDGEMENT

This work is supported by the National Natural Science Foundation of China (Grant Nos. U22A20242 and 52371263**).**

REFERENCES

[1] Wilks, B., Montiel, F., & Wakes, S. (2022). Rainbow reflection and broadband energy absorption of water waves by graded arrays of vertical barriers. *Journal of Fluid Mechanics*, 941, A26.

[2] Tsakmakidis, K. L., Boardman, A. D., & Hess, O. (2007). 'Trapped rainbow'storage of light in metamaterials. *Nature*, 450(7168), 397-401.

[3] Zhu, J., Chen, Y., Zhu, X., Garcia-Vidal, F. J., Yin, X., Zhang, W., & Zhang, X. (2013). Acoustic rainbow trapping. *Scientific reports*, 3(1), 1728.

[4] Skelton, E. A., Craster, R. V., Colombi, A., & Colquitt, D. J. (2018). The multi-physics metawedge: graded arrays on fluid-loaded elastic plates and the mechanical analogues of rainbow trapping and mode conversion. *New Journal of Physics*, 20(5), 053017.

[5] Colombi, A., Colquitt, D., Roux, P., Guenneau, S., & Craster, R. V. (2016). A seismic metamaterial: The resonant metawedge. *Scientific reports*, 6(1), 27717.

[6] Bennetts, L. G., Peter, M. A., & Craster, R. V. (2018). Graded resonator arrays for spatial frequency separation and amplification of water waves. *Journal of Fluid Mechanics*, 854, R4.

[7] Peter, M. A. (2018). Rainbow trapping of water waves. *The 33th International Workshop on Water Waves and Floating Bodies*, Guidel-Plages, France.

[8] Archer, A. J., Wolgamot, H. A., Orszaghova, J., Bennetts, L. G., Peter, M. A., & Craster, R. V. (2020). Experimental realization of broadband control of water-wave-energy amplification in chirped arrays. *Physical Review Fluids*, 5(6), 062801.

[9] Dupont, G., Remy, F., Kimmoun, O., Molin, B., Guenneau, S., & Enoch, S. (2017). Type of dike using C-shaped vertical cylinders. *Physical Review B*, 96(18), 180302.

[10] Hu, X., Yang, J., Zi, J., Chan, C. T., & Ho, K. M. (2013). Experimental observation of negative effective gravity in water waves. *Scientific reports*, 3(1), 1916.